Journal of Robotics, Networking and Artificial Life
Vol. **8**(**2**); September (2021), *pp.* 127–133
DOI: https://doi.org/10.2991/jrnal.k.210713.012; ISSN 2405-9021; eISSN 2352-6386
https://www.atlantis-press.com/journals/jrnal

Research Article

# A No-Reference Image Quality Assessment Metric for Wood Images

Heshalini Rajagopal[1,*], Norrima Mokhtar[1], Anis Salwa Mohd Khairuddin[1], Wan Khairunizam[2], Zuwairie Ibrahim[3], Asrul Bin Adam[3], Wan Amirul Bin Wan Mohd Mahiyidin[1]

[1]*Department of Electrical Engineering, Faculty of Engineering, University of Malaya, Malaysia*
[2]*School of Mechatronic Engineering, University of Malaysia Perlis, Malaysia*
[3]*College of Engineering, University of Malaysia Pahang, Malaysia*

**ARTICLE INFO**

*Article History*

Received 19 October 2020
Accepted 01 June 2021

*Keywords*

Wood images
GLCM
Gabor
GGNR-IQA
NR-IQA

**ABSTRACT**

Image Quality Assessment (IQA) is a vital element in improving the efficiency of an automatic recognition system of various wood species. There is a need to develop a No-Reference IQA (NR-IQA) system as a perfect and distortion free wood images may be impossible to be acquired in the dusty environment in timber factories. To the best of our knowledge, there is no NR-IQA developed for wood images specifically. Therefore, a Gray Level Co-Occurrence Matrix (GLCM) and Gabor features-based NR-IQA (GGNR-IQA) metric is proposed to assess the quality of wood images. The proposed metric is developed by training the support vector machine regression with GLCM and Gabor features calculated for wood images together with scores obtained from subjective evaluation. The proposed IQA metric is compared with a widely used NR-IQA metric, Blind/Referenceless Image Spatial Quality Evaluator (BRISQUE) and Full Reference-IQA (FR-IQA) metrics. Results shows that the proposed NR-IQA metric outperforms the BRISQUE and the FR-IQA metrics. Moreover, the proposed NR-IQA metric is beneficial in wood industry as a distortion free reference image is not needed to evaluate the wood images.

© 2021 *The Authors*. Published by Atlantis Press International B.V.
This is an open access article distributed under the CC BY-NC 4.0 license (http://creativecommons.org/licenses/by-nc/4.0/).

## 1. INTRODUCTION

Wood is extensively used for furniture, building construction and paper production [1]. There are various types of wood and each of them has different attributes with regard to its formation, thickness, color and texture [2]. These varying characteristics defines their ideal usages and economic values [3]. As the price and characteristics of every wood species differs, misclassification may cause financial losses. Hence, there is a need to identify different wood species accurately.

Conventionally, the recognition of wood species is performed manually by human subjects [4]. However, this practice is time and cost consuming to the lumber industry. Hence, several automatic wood species recognition systems have been developed [1,2,5,6]. The efficiency of automatic wood recognition systems can be improved by using superior quality microscopy images which are commonly enhanced to improve the rate of successful wood species recognition. Nevertheless, the image enhancement processes consume extra computational time, and could cause a checkerboard artefact to the wood images [7]. In addition, the dusty and dark environment in timber factories could degrade the quality of the image acquired [8]. Thus, an appropriate Image Quality Assessment (IQA) algorithm is required to assess the acquired wood images prior to feeding it to any automatic wood recognition system.

Image quality assessment can be categorized into subjective and objective evaluations. Subjective evaluation is the scores given by human subjects based on their judgment on the image quality. While, objective evaluation is done based on numerical methods to determine the quality of the images. Even though, subjective evaluation is the benchmark of IQA, it is impracticable in an industrial environment as it is time and cost consuming. Therefore, it is necessary to develop an objective evaluation procedures that is capable to imitate subjective IQA evaluation [9].

Objective evaluation can be categorized into Full-Reference-IQA (FR-IQA) [10–15], Reduced Reference-IQA (RR-IQA) [16,17] and No-Reference/Blind IQA (NR-IQA) [18–20]. FR-IQA uses the reference image fully to assess the images [10–15] whereas RR-IQA uses the reference images partially [16,17]. In contrast, NR-IQA assesses an image without using a reference image [18–21]. NR-IQA is the most appropriate algorithm to evaluate the quality of the wood images as it may be impossible to obtain high quality images in the dusty and dark setting of lumber factories. Therefore, we propose the Gray Level Co-Occurrence Matrix (GLCM) and Gabor features-based NR-IQA, GGNR-IQA algorithm to evaluate wood images.

The GLCM and Gabor features are widely used in wood species recognition system [5,22–24]. The proposed GGNR-IQA algorithm is compared with a commonly utilized NR-IQA, Blind/Referenceless Image Spatial Quality Evaluator (BRISQUE) [18], and FR-IQAs namely, Structural Similarity Index (SSIM) [10],

*Corresponding author. Email: heshalini@gmail.com

Multiscale SSIM (MS-SSIM) [10], Feature Similarity (FSIM) [11], Information Weighted SSIM (IW-SSIM) [12] and Gradient Magnitude Similarity Deviation (GMSD) [13]. There is significant difference between the proposed GGNR-IQA between the BRISQUE. Technically, BRISQUE is generalized to evaluate natural images and is not suitable to assess the wood images while the proposed GGNR-IQA is trained to assess the wood images. The performances of the GGNR-IQA, BRISQUE and FR-IQAs are evaluated by using the Pearson Linear Correlation Coefficient (PLCC) and Root Mean Squared Error (RMSE) computed between the human Mean Opinion Scores (MOS) and the algorithms.

## 2. MATERIALS AND METHODS

### 2.1. Training and Testing Database

An Support Vector Machine Regression (SVR) model is trained with the 44 features of GLCM and Gabor calculated for normalized wood images with the human MOS which are obtained from the subjective evaluation for wood images. The MOS, GLCM and Gabor features are utilized as the training and testing database to obtain an optimized SVR model. The SVM model is used widely in modelling IQA metric as it is capable to handle high-dimensional data exist along with a corresponding lack of knowledge of the underlying distribution. Even with a relatively small sample size, SVMs have the benefit of not being constrained by distributional assumptions, other than that the data are independent and identically distributed [25].

#### 2.1.1. Wood images

Ten wood images from various wood genus, as shown in Figure 1 were chosen. The images were acquired from a wood database: https://www.wood-database.com/ [26]. The images were converted to grayscale and the pixel values were normalized to the range 0–255 for ease of applying the same levels of distortion across all the reference images. The images consisted of a matrix of 600 × 600 pixels, corresponding to resolution of 360,000 and an image area of 9525 cm$^2$. The 10 reference images were distorted by Gaussian white noise and motion blur. These two types of distortions usually occur in the industrial setting. Generally, the wood images are exposed to Gaussian white noise due to the poor illumination and heat in the lumber mill while acquiring the wood images [8,27].

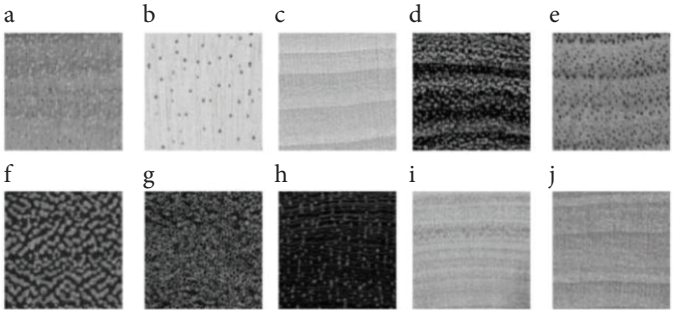


**Figure 1** | Ten wood images used as reference images (a) *Turraeanthus africanus*, (b) *Ochroma pyramidale*, (c) *Tilia americana*, (d) *Cordia* spp., (e) *Juglans cinerea*, (f) *Vouacapoua americana*, (g) *Dipterocarpus* spp., (h) *Swartzia cubensis*, (i) *Cordia* spp., (j) *Cornus florida*.

On the other hand, wood images are exposed to motion blur when there is a relative motion between the wood slice and camera [6].

These distortions degrade the quality of the wood images where the features of the pores on the wood texture may not be discerned. Hence, this may lead to misclassification of the wood genus as the feature extractor may not obtain distinctive features from the wood images efficiently [28]. Nine modulations of Gaussian white noise with standard deviation, $\sigma_{GN}$ and motion blur with standard deviation, $\sigma_{MB}$ were added to the reference images, i.e.: $\sigma_{GN}$ = 10, 20, 30, 40, 50, 60, 70, 80 and 90 for Gaussian white noise and $\sigma_{MB}$ = 2, 4, 6, 8, 10, 12, 14, 16 and 18 for motion blur.

#### 2.1.2. GLCM and gabor features

First, Mean Subtracted Contrast Normalized (MSCN), $\hat{I}(m,n)$ is calculated from the wood image, $I(m,n)$ using Equation (1) [18]:

$$\hat{I}(m,n) = \frac{I(m,n) - \mu(m,n)}{\sigma(m,n) + 1} \tag{1}$$

where $\mu(m,n)$ and $\sigma(m,n)$ denote the mean and variance of wood image, $I(m,n)$, respectively, $m \in 1, 2, ..., M$, $n \in 1, 2, ..., N$ are spatial indices while $M$ represents the height and $N$ represents width of image, $I(m,n)$.

The mean, $\mu(m,n)$ and variance, $\sigma(m,n)$ of the wood image are computed using Equations (2) and (3), respectively [18]:

$$\mu(m,n) = \sum_{k=-K}^{K}\sum_{l=-L}^{L} w_{k,l} I_{k,l}(m,n) \tag{2}$$

$$\sigma(m,n) = \sqrt{\sum_{k=-K}^{K}\sum_{l=-L}^{L} w_{k,l}(I_{k,l}(m,n) - \mu(m,n))^2} \tag{3}$$

Where $w = \{w_{k,l} \mid k = -K,\ldots,K, l = -L,\ldots,L\}$ is a 2-dimensional (2D) circularly-symmetric Gaussian weighting function that is sampled out to three standard deviations and rescaled to unit volume, and $K$ and $L$ represent the window sizes.

The MSCN coefficients, $\hat{I}(m,n)$ highlights the main features of the wood images such as pores and grains, with few low-energy residual object boundaries [21]. Therefore, the MSCN is used to compute the GLCM and Gabor features instead of the image, $I(m,n)$. Next, two types of features namely, GLCM and Gabor features were incorporated in this study.

##### 2.1.2.1. GLCM features

The GLCM depicts second order statistical analysis of an image by analyzing how often the pairs of pixels which consist of specific values and spatial relationship take place in an image. The probability, $p(m, n)$ is computed using Equation (4) [29]:

$$p(m, n) = \{C(m, n) \mid (d, \theta)\} \tag{4}$$

where $d$ is the inter-pixels displacement distance, $\theta$ denotes orientation and $C(m,n)$ denotes the frequency of gray level occurrence in MSCN of the image, $\hat{I}(m,n)$. Four statistical textures such as

contrast, correlation, energy, and homogeneity were extracted from the GLCM matrix.

Contrast calculates the local variations in the GLCM and is defined as Equation (5) [29]:

$$\text{Contrast} = \sum_{m,n} |m-n|^2 \, p(m,n) \tag{5}$$

Correlation computes the joint probability occurrence of the specified pixel pairs and is defined as Equation (6) [29]:

$$\text{Correlation} = \sum_{m,n} \frac{(m-\mu m)(n-\mu n)p(m,n)}{\sigma_m \sigma_n} \tag{6}$$

Energy calculates the sum of squared components in the GLCM. It is also known as uniformity or the angular second moment. The energy parameter is computed as Equation (7) [29]:

$$\text{Energy} = \sum_{m,n} p(m,n)^2 \tag{7}$$

Homogeneity calculates the closeness of the distribution of elements in the GLCM to the GLCM diagonal and is computed as Equation (8) [29]:

$$\text{Homogeneity} = \sum_{m,n} \frac{p(m,n)}{1+|m-n|} \tag{8}$$

These four parameters were computed at four directions, 0°, 45°, 90° and 135° and this form 16 GLCM features.

#### 2.1.2.2. Gabor features

The 2D Gabor function which represents the spatial summation properties of simple cells in the visual cortex and it is defined as Equation (9) [30]:

$$g(x,y;\lambda,\theta,\psi,\sigma,\gamma) = \exp\left(-\frac{x'^2+\gamma^2 y'^2}{2\sigma^2}\right)\cos\left(2\pi\frac{x'}{\lambda}+\psi\right) \tag{9}$$

where

$$x' = x\cos\theta + y\sin\theta \tag{10}$$

$$y' = -x\sin\theta + y\cos\theta \tag{11}$$

$\lambda$ denotes the wavelength of the sinusoidal factor, $\theta$ denotes the orientation of the normal to the parallel stripes of a Gabor function, $\psi$ represents the phase offset, $\sigma$ represents the standard deviation of the Gaussian envelope and $\gamma$ represents the spatial aspect ratio.

The computational models of 2D Gabor filters are defined in Equations (12) and (13) [30]:

$$h_e = g(x,y)\cos(2\pi f(x\cos\theta + y\sin\theta)) \tag{12}$$

$$h_o = g(x,y)\sin(2\pi f(x\cos\theta + y\sin\theta)) \tag{13}$$

where $h_e$ and $h_o$ represents the even symmetric and odd symmetric Gabor filters, respectively and $g(x,y)$ represents the isotropic Gaussian function and is computed as Equation (14) [30]:

$$g(x,y) = \frac{1}{\sqrt{2\pi\sigma^2}}\exp\left(-\frac{x'^2+y'^2}{2\sigma^2}\right) \tag{14}$$

And the spatial frequency response of the Gabor functions, $f$ is as shown in Equation (15) [30]:

$$f = N/P \tag{15}$$

where $N$ denotes the size of the kernel and $P$ denotes period in pixel.

In this study, wavelength, $\lambda$ is in increasing powers of two starting from $4/\sqrt{2}$ up to the hypotenuse length of the input image [31] and this produces seven Gabor features. The seven Gabor features were then computed in four orientations, 0°, 45°, 90° and 135°, similar to the GLCM computations. This forms 28 features Gabor features. In total, the 16 GLCM and 28 Gabor features were combined and this forms 44 features. These 44 features were calculated using the MSCN coefficients, $\hat{I}(m,n)$ and are used to train SVR.

### 2.1.3. MOS

The MOS values were obtained from subjective evaluation participated by 10 students aged between 20 and 25 years from Manipal International University (MIU), Malaysia. The evaluation was carried out as per the procedures suggested in Rec. ITU-R BT.500-11 [32] where it was performed in an office environment using a 21-inch LED computer screen.

Simultaneous double stimulus for continuous evaluation approach was used in this evaluation [32,33] where the reference and distorted images are shown side-by-side on the computer screen and each subject compares the quality of the images displayed on the right side with its reference image (left side) to evaluate the displayed image.

The score given by the human subjects are either Excellent (5), Good (4), Fair (3), Poor (2) or Bad (1) for each image displayed. The evaluation process takes 15–20 min for each subject. The scores obtained from the subjects were averaged to convert them to the MOS [34]. These MOS values are also used to train SVR.

### 2.1.4. Support vector machine regression

$\epsilon$-Support Vector Machine Regression (SVR) [35] is trained using MOS and 44 GLCM and Gabor features of wood images in this study. The 44 image features (GLCM and Gabor features) calculated for the wood images are mapped to the MOS values of the corresponding wood images. The 44 GLCM and Gabor features and MOS of wood images were randomly split into training and testing sets where 80% of the 44 features and MOS values were used to train the SVR model to obtain an SVR model with optimized parameters and 20% were utilized to evaluate the optimized SVR model. There was no overlap between the training and testing data

to ensure a fair prediction of quality scores. Several experiments were performed on the training and testing data split (70% for training and 30% for testing, 80% for training and 20% for testing and 90% for training and 10% for testing). When a higher percentage of data (90%) for training procedure was tested, the model performance only increased slightly. However, the computation time is longer. A lower percentage of data (70%) for training procedure was tested but the performance of the model decreased. Hence, 80% of data was used for training and 20% of data was used for testing the model.

The flow diagram of the proposed GGNR-IQA is shown in Figure 2. The performance of GGNR-IQA was evaluated using PLCC [36] and RMSE [37] calculated between 1000 iterations were performed on the training and testing of the SVR model to obtain an optimized SVR model. The cost parameter, $C$, and width parameter, $g$, of the optimized SVR model are 32,768 and 0.125, respectively.

## 2.2. Performance Evaluation

The proposed GGNR-IQA is compared with a well-known NR-IQA algorithm, BRISQUE and five FR-IQAs [28]: SSIM [10], MS-SSIM [10], FSIM [11], IW-SSIM [12] and GMSD [13].

The performance of the GGNR-IQA, BRISQUE and FR-IQAs is assessed using PLCC and RMSE [33] values calculated between these algorithms and MOS.

## 3. RESULTS AND DISCUSSION

The efficiency of the GGNR-IQA was further assessed using a second dataset which was generated from the same wood image database [26]. This second dataset was produced using 10 reference images acquired from 10 various wood genus as shown in Figure 3.

These reference images were added with the similar distortion type (Gaussian white noise and motion blur) and modulations as the training and testing database. This means that the second dataset includes 10 reference images and 180 distorted images.

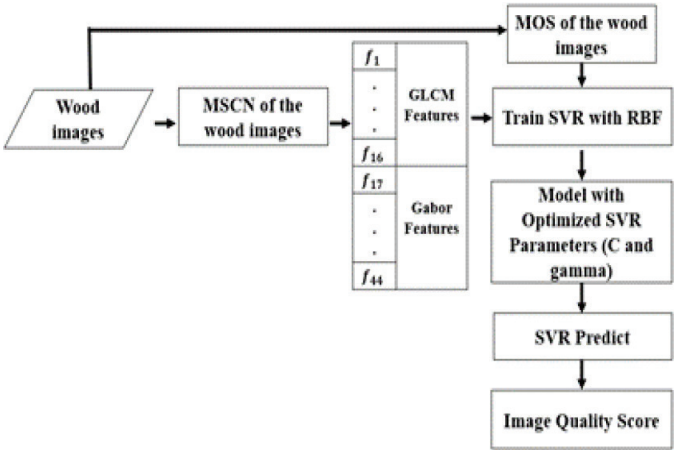


**Figure 2** | Flow diagram of the proposed GGNR-IQA.

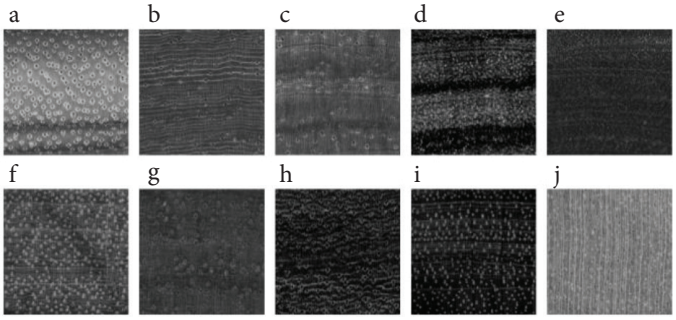


**Figure 3** | Reference wood images in the second dataset (a) *Julbernardia pellegriniana*, (b) *Dalbergia cultrate*, (c) *Dalbergia retusa*, (d) *Dalbergia cearensis*, (e) *Guaiacum officinale*, (f) *Swartzia* spp., (g) *Dalbergia spruceana*, (h) *Dalbergia sissoo*, (i) *Swartzia benthamiana* and (j) *Euxylophora paraensis.*

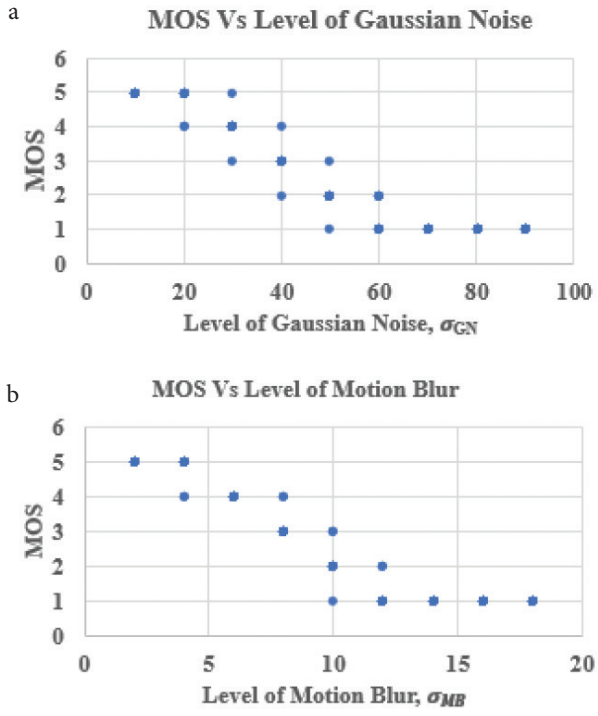


**Figure 4** | Scatter Plot of MOS versus nine distortion modulations of (a) Gaussian white noise and (b) motion blur.

## 3.1. Relationship between MOS and Quality of Image with Different Distortion Modulations

Figure 4a and 4b shows the correlation between MOS and nine distortion modulations of Gaussian white noise and motion blur. Lower MOS values show lower image quality which is caused by higher distortion modulation. On the other hand, higher MOS values represent higher image quality which is generated by lower distortion modulation. Based on Figure 4a and 4b, the MOS decreases as the distortion modulation increases. This means that all the human subjects could discern the images distorted with the various modulations of Gaussian white noise and motion blur.

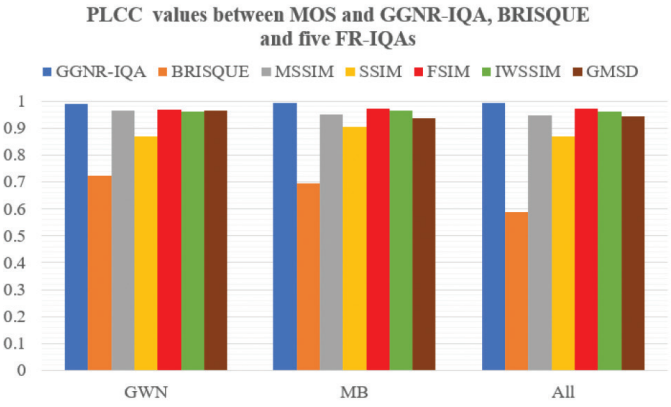


**Figure 5** | PLCC values between GGNR-IQA, BRISQUE, FR-IQAs and MOS.

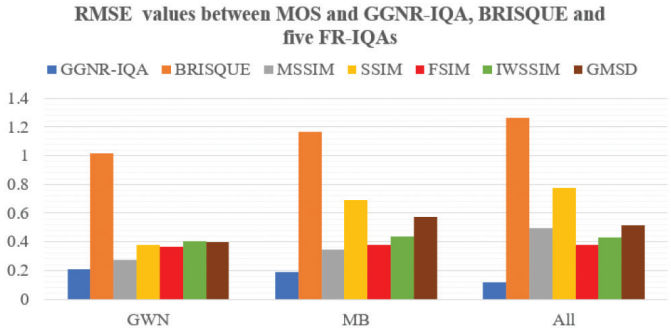


**Figure 6** | RMSE values between GGNR-IQA, BRISQUE, FR-IQAs and MOS.

### 3.2. Correlation between GGNR-IQA, BRISQUE and FR-IQAs Algorithms and MOS

The PLCC and RMSE values calculated between MOS and the proposed GGNR-IQA metric, BRISQUE and the five FR-IQA metrics are shown in Figures 5 and 6, respectively. The most suitable IQA for wood images is expected to have the highest PLCC and lowest RMSE values. Figure 5 shows that the PLCC values obtained for the GGNR-IQA for Gaussian white noise, motion blur and the overall database are the highest compared to the BRISQUE and FR-IQAs. This shows that the GGNR-IQA algorithm outperforms BRISQUE and all the five FR-IQAs. This is further proved with the lowest RMSE values for the proposed metric compared to BRISQUE and all the five FR-IQAs as shown in Figure 6.

## 4. CONCLUSION

A NR-IQA algorithm, GGNR-IQA was proposed to assess wood images prior to feeding the image to wood species classification and recognition system. The proposed GGNR-IQA algorithm was trained using GLCM, Gabor features and MOS obtained from wood images. The performance of the GGNR-IQA algorithm was assessed by comparing the PLCC and RMSE values calculated between GGNR-IQA, BRISQUE, five FR-IQA algorithms and MOS. PLCC and RMSE values showed that the GGNR-IQA algorithm outperforms BRISQUE and all the five FR-IQAs. This shows that the GGNR-IQA algorithm could assess the quality of wood images accurately. In addition, the proposed GGNR-IQA algorithm would not require a distortion free reference image to determine the quality of the wood images. This is beneficial especially when it is impossible to obtain a distortion free reference image in the dusty environment of lumber mill.

## CONFLICTS OF INTEREST

The authors declare they have no conflicts of interest.

## REFERENCES

[1] S. Shivashankar, M.R. Kagale, Automatic wood classification using a novel color texture features, Int. J. Comput. Appl. 180 (2018), 34–38.
[2] P. Barmpoutis, K. Dimitropoulos, I. Barboutis, N. Grammalidis, P. Lefakis, Wood species recognition through multidimensional texture analysis, Comput. Electron. Agric. 144 (2018), 241–248.
[3] M.I.P. Zamri, F. Cordova, A.S.M. Khairuddin, N. Mokhtar, R. Yusof, Tree species classification based on image analysis using Improved-Basic Gray Level Aura Matrix, Comput. Electron. Agric. 124 (2016), 227–233.
[4] R. Gazo, L. Wells, V. Krs, B. Benes, Validation of automated hardwood lumber grading system, Comput. Electron. Agric. 155 (2018), 496–500.
[5] S. Mohan, K. Venkatachalapathy, P. Sudhakar, An intelligent recognition system for identification of wood species, J. Comput. Sci. 10 (2014), 1231–1237.
[6] C. Guang-Sheng, Z. Peng, Dynamic wood slice recognition using image blur information, Sens. Actuat. A Phys 176 (2012), 27–33.
[7] B. Xiao, H. Tang, Y. Jiang, W. Li, G. Wang, Brightness and contrast controllable image enhancement based on histogram specification, Neurocomputing 275 (2018), 2798–2809.
[8] J. Ratnasingam, F. Ioras, T.T. Swan, C.Y. Yoon, G. Thanasegaran, Determinants of occupational accidents in the woodworking sector: the case of the Malayasian wooden furniture industry, J. Appl. Sci. 11 (2011), 561–566.
[9] Z. Wang, Applications of objective image quality assessment methods, IEEE Signal Process Mag. 28 (2011), 137–142.
[10] Z. Wang, E.P. Simoncelli, A.C. Bovik, Multiscale structural similarity for image quality assessment, 37th Asilomar Conference on Signals, Systems and Computers, IEEE, Pacific Grove, CA, USA, 2003, pp. 1398–1402.
[11] L. Zhang, L. Zhang, X. Mou, D. Zhang, FSIM: a feature similarity index for image quality assessment, IEEE Trans. Image Process. 20 (2011), 2378–2386.
[12] Z. Wang, Q. Li, Information content weighting for perceptual image quality assessment, IEEE Trans Image Process. 20 (2011), 1185–1198.
[13] W. Xue, L. Zhang, X. Mou, A.C. Bovik, Gradient magnitude similarity deviation: a highly efficient perceptual image quality index, IEEE Trans. Image Process. 23 (2014), 684–695.
[14] M. Gulame, K.R. Joshi, R.S. Kamthe, A full reference based objective image quality assessment, Int. J. Adv. Electr. Electron. Eng. 2 (2013), 13–18.
[15] D.M. Chandler, Seven challenges in image quality assessment: past, present, and future research, ISRN Signal Process. 2013 (2013), 1–53.

[16] U. Engelke, M. Kusuma, H.J. Zepernick, M. Caldera, Reduced-reference metric design for objective perceptual quality assessment in wireless imaging, Signal Process. Image Commun. 24 (2009), 525–547.
[17] D.V.M. Zhou Wang, E.P. Simoncelli, Reduced-reference image quality assessment using a wavelet-domain natural image statistic model, Proceedings of the SPIE 5666, Human Vision and Electronic Imaging X, Society of Photo-Optical Instrumentation Engineers (SPIE), San Jose, California, United States, 2005.
[18] A. Mittal, A.K. Moorthy, A.C. Bovik, No-reference image quality assessment in the spatial domain, IEEE Trans. Image Process. 21 (2012), 4695–4708.
[19] W. Zhang, K. Ma, J. Yan, D. Deng, Z. Wang, Blind image quality assessment using a deep bilinear convolutional neural network, IEEE Trans. Circuits Syst. Video Technol. 30 (2018), 36–47.
[20] S. Bosse, D. Maniry, K.R. Müller, T. Wiegand, W. Samek, Deep neural networks for no-reference and full-reference image quality assessment, IEEE Trans. Image Process. 27 (2017), 206–219.
[21] H. Rajagopal, N. Mokhtar, T.F.T.M.N. Izam, W.K.W. Ahmad, No-reference quality assessment for image-based assessment of economically important tropical woods, PLoS One 15 (2020), e0233320.
[22] M. Khalid, E.L.Y. Lee, R. Yusof, M. Nadaraj, Design of an intelligent wood species recognition system, Int. J. Simul. Syst. Sci. Technol. 9 (2008), 9–19.
[23] J.Y. Tou, Y.H. Tay, P.Y. Lau, A comparative study for texture classification techniques on wood species recognition problem, 2009 Fifth International Conference on Natural Computation, IEEE, Tianjian, China, 2009, pp. 8–12.
[24] R. Bremananth, B. Nithya, R. Saipriya, Wood species recognition using GLCM and correlation, 2009 International Conference on Advances in Recent Technologies in Communication and Computing, IEEE, Kottayam, India, 2009, pp. 615–619.
[25] M.D. Wilson, Support vector machines, in: S.E. Jørgensen, B.D. Fath (Eds.), Encyclopedia of Ecology, Academic Press, Oxford, 2008, pp. 3431–3437.
[26] E. Meier, The Wood Database, 2007. Accessed August 16, 2018.
[27] T. Rahman, M.R. Haque, L.J. Rozario, M.S. Uddin, Gaussian noise reduction in digital images using a modified fuzzy filter, 2014 17th International Conference on Computer and Information Technology (ICCIT), IEEE, Dhaka, Bangladesh, 2014, pp. 217–222.
[28] H. Rajagopal, A.S. Khairuddin, N. Mokhtar, A. Ahmad, R. Yusof, Application of image quality assessment module to motion-blurred wood images for wood species identification system, Wood Sci. Technol. 53 (2019), 967–981.
[29] M.H. Abd Latif, H.Md. Yusof, S.N. Sidek, N. Rusli, Implementation of GLCM features in thermal imaging affective state detection, Procedia Com. Sci. 76 (2015), 308–315.
[30] R. Yusof, N.R. Rosli, M. Khalid, Using Gabor filters as image multiplier for tropical wood species recognition system, 2010 12th International Conference on Computer Modelling and Simulation, IEEE, Cambridge, UK, 2010, pp. 289–294.
[31] A.K. Jain, F. Farrokhnia, Unsupervised texture segmentation using Gabor filters, Pattern Recognit. 24 (1991), 1167–1186.
[32] Recommendation ITU-R BT.500-11. Methodology for the subjective assessment of the quality of television pictures, 2000.
[33] L.S. Chow, H. Rajagopal, R. Paramesran, Alzheimer's Disease Neuroimaging Initiative, Correlation between subjective and objective assessment of magnetic resonance (MR) images, Magn. Reson. Imaging 34 (2016), 820–831.
[34] L.S. Chow, H. Rajagopal, Modified-BRISQUE as no reference image quality assessment for structural MR images, Magn. Reson. Imaging 43 (2017), 74–87.
[35] C.C. Chang, C.J. Lin, LIBSVM: a library for support vector machines, ACM Trans. Intell. Syst. Technol. 2 (2011), 1–27.
[36] X.K. Song, Correlated Data Analysis: Modelling, Analytics, and Applications, Springer Science & Business Media, Springer-Verlag, New York, 2007.
[37] T. Chai, R.R. Draxler, Root mean square error (RMSE) or mean absolute error (MAE)? – Arguments against avoiding RMSE in the literature, Geosci. Model Dev. 7 (2014), 1247–1250.

## AUTHORS INTRODUCTION

**Ms. Heshalini Rajagopal**

She received her Master's degree from the Department of Electrical Engineering, University of Malaya, Malaysia in 2016. She has passed her PhD Viva Voce in University of Malaya, Malaysia recently. She received the B.E. (Electrical) in 2013 and MEngSc in 2016 from University of Malaya, Malaysia. Currently, she is a lecturer in Manipal International University, Nilai, Malaysia. Her research interests include image processing, artificial intelligence and machine learning.

**Dr. Norrima Mokhtar**

She received the B.Eng. degree from University of Malaya, the M.Eng. and the PhD degree from Oita Univerity, Japan. She is currently a senior lecturer in the Department of Electrical Engineering, University of Malaya. Her research interests are signal processing and human machine interface.

**Dr. Anis Salwa Mohd Khairuddin**

She received PhD in computer engineering at Universiti Teknologi Malaysia (UTM). She received the B.Eng. (Hons) Electrical and Electronics Engineering from Universiti Tenaga Nasional, Malaysia, in 2007 and Masters degree in computer engineering from Royal Melbourne Institute of Technology, Australia, in 2009. She is currently a Senior Lecturer from University of Malaya. Her current interests include pattern recognition, image analysis, and artificial intelligence.

**Dr. Asrul Bin Adam**

He received the B.Eng. and M.Eng. degrees in Electrical-Mechatronics and Electrical Engineering from Universiti Teknologi Malaysia (UTM), Malaysia, in 2009 and 2012, respectively. He completed his PhD in Signal and System from Faculty of Engineering, University of Malaya in 2017. He currently works as lecturer at Faculty of Manufacturing Engineering, Universiti Malaysia Pahang, Malaysia. His research interests include biomedical signals processing, artificial intelligent, machine learning, and optimization.

**Dr. Wan Khairunizam**

He received his B.Eng. degree in Electrical & Electronic Engineering from Yamaguchi University and PhD in Intelligent Mechanical System Engineering from Kagawa University, Japan in 1999 and 2009 respectively. He is currently an Associate Professor of Mechatronic at School of Mechatronic Engineering, University Malaysia Perlis (UniMAP), Malaysia. His specialties are in Human-Computer Interaction, Intelligent Transportation System (ITS), Artificial Intelligence (AI) and Robotics.

**Dr. Wan Amirul Bin Wan Mohd Mahiyidin**

He received the M.Eng. degree from the Imperial College London in 2009, the M.Sc. degree from University of Malaya in 2012, and the PhD degree from University of Canterbury in 2016. He is currently a senior lecturer at the Department of Electrical Engineering, University of Malaya. His research interests are multiple antennas system, cooperative MIMO, channel modelling and positioning system.

**Dr. Zuwairie Ibrahim**

He received his B.Eng. (Mechatronics) and M.Eng. (Image Processing) from Universiti Teknologi Malaysia, in 2000 and 2002, respectively. In 2006, he has been awarded a PhD (DNA Computing) from Meiji University, Japan. He is currently an Associate Professor in the Faculty of Electrical and Electronic Engineering, Universiti Malaysia Pahang. His research interests include computational intelligence, image processing, and unconventional computation such as molecular or DNA computing.